$p = 2.5$.

As presented in this Letter, the Schwinger method for the multichannel scattering has been shown to yield much better results than those of other variational methods. The rapid convergence is dramatic. In conclusion, the Schwinger variational principle is quite promising and encouraging for the multichannel scattering as well as for the single-channel case.

Recently Thirumalai and Truhlar[13] carried out a series of calculations on an attractive exponential potential which were designed to compare the convergence of the Schwinger variational principle with that of the Kohn method. They concluded that the Kohn-type methods show much better convergence to the accurate result than the Schwinger method. Unfortunately the same trial scattering wave functions were not used in these two variational principles. We have repeated these calculations using the same trial wave functions in the Schwinger and Kohn variational principles and find that the Schwinger procedure gives superior results.[14] Hence these results are in fact consistent with the trend seen in the present application of these methods to this two-channel model problem. Details of these calculations and a discussion of the mathematical relationship between the Schwinger and Kohn variational methods will be published elsewhere.[14]

[1]J. M. Blatt and J. D. Jackson, Phys. Rev. 76, 18 (1949).
[2]A. L. Zubarev, Fiz. Elem. Chastis At. Yadra 9, 453 (1978) [Sov. J. Part. Nucl. 9, 188 (1978)].
[3]D. K. Watson and V. McKoy, Phys. Rev. A 20, 1474 (1979).
[4]R. R. Lucchese and V. McKoy, J. Phys. B 12, L421 (1979).
[5]R. R. Lucchese and V. McKoy, Phys. Rev. A 21, 112 (1980).
[6]D. K. Watson, R. R. Lucchese, V. McKoy, and T. N. Rescigno, Phys. Rev. A 21, 738 (1980).
[7]R. R. Lucchese, D. K. Watson, and V. McKoy, Phys. Rev. A 22, 421 (1980).
[8]R. J. Huck, Proc. Phys. Soc. London, Sect. A 70, 369 (1957).
[9]R. K. Nesbet, Phys. Rev. 179, 60 (1969).
[10]R. K. Nesbet and R. S. Oberoi, Phys. Rev. A 6, 1855 (1972).
[11]R. K. Nesbet, Phys. Rev. A 18, 955 (1978).
[12]F. E. Harris and H. H. Michels, Phys. Rev. Lett. 22, 1036 (1969).
[13]D. Thirumalai and D. G. Truhlar, Chem. Phys. Lett. 70, 330 (1980).
[14]K. Takatsuka, R. R. Lucchese, and V. McKoy, "The Relationship Between the Schwinger and Kohn-type Variational Principles in Scattering Theory" (to be published).

Heating by Raman Backscatter and Forward Scatter

Kent Estabrook, W. L. Kruer, and B. F. Lasinski

Lawrence Livermore Laboratory, University of California, Livermore, California 94550

This Letter presents computer simulations of the reflection and heating due to stimulated Raman scattering of intense laser light in large regions of underdense plasma. The heated electron distribution is approximately a Maxwellian of temperature $\frac{1}{2}m_e v_p^2$. A simple model of the reflection is presented. Forward Raman scattering was also observed producing extremely energetic electrons. Finally, two-dimensional simulations showed sizable Raman scattering coexisting with heating by the $2\omega_{pe}$ instability. Raman scattering may cause a preheat problem with large laser-fusion-reactor targets.

Motivated by recent observations[1,2] of Raman scattering in reactor targets and the great interest in this process as a preheat source, we present computer simulations of the reflection and heating due to stimulated Raman backscattering of intense laser light in large regions of under-

dense plasma. Stimulated Raman scattering[3,4] is the parametric decay of an incident photon into a scattered photon plus a longitudinal electron plasma wave (epw). The frequency matching conditions are $\omega_0 \to \omega_s + \omega_{epw}$, where ω_0 (ω_s) is the angular frequency of the incident (reflected) light wave and ω_{epw} is the frequency of the electron plasma wave. As can be seen from the frequency-matching condition, this process can occur for electron densities $n \lesssim n_{cr}/4$, where n_{cr} is the critical density. The Raman process is a resonant, absolute[4] instability for $n \approx n_{cr}/4$ and occurs most efficiently at that density. The absorption may be more if the backscattered (forward-scattered) light is subsequently absorbed. As the density decreases, the backscattered epw wavelength λ_{epw} becomes shorter with respect to the laser wavelength and in particular with respect to the Debye length $\lambda_D = (T_e/4\pi n e^2)^{1/2}$, where T_e (e) is the electron temperature (charge). The electron Landau damping becomes considerable for $\lambda_{epw} \lesssim 10\lambda_D$, which occurs for high electron temperatures and low densities ($n/n_{cr} \lesssim 0.01T_e$). Here the instability is a variation of Raman scattering called stimulated Compton scattering. There is also an intermediate regime for densities $< 0.25 n_{cr}$ for which the instability is convective, moderately damped, and can still absorb and scatter a significant amount of light. The convective regime deserves special attention since it is not restricted to a narrow range of densities near $n_{cr}/4$. We concentrate on the convective instability to provide initial estimates for target design and will

later briefly discuss the more complex region near quarter critical at which the Raman instability is absolute and where the $2\omega_{pe}$ instability also occurs. The Raman instability is an important consideration for reactor targets since these targets will be characterized by large regions of underdense plasma. The most critical feature of the Raman backscattering (forward scattering) is its ability to generate high-energy electrons,[1] which may lead to significant preheat. Both forward scattering and backscattering accelerate electrons in the direction of the laser. The back and forward refer to the direction of the scattered light.

The simulations were $1\frac{1}{2}$ and 2 dimensional, kinetic (particle in cell), electromagnetic, and performed with relativistic electrons. The light boundary condition allows the light to pass through each end as in vacuum. Particles leaving the boundary were reemitted back into the plasma with the initial temperature. Figure 1 shows the hot-electron distribution observed in a sample computer simulation. Note the high-energy electron tail which is generated by the electron plasma wave as it damps. This tail is roughly Maxwellian in shape and has a temperature of 13 keV.

FIG. 1. Particle number vs energy showing the Maxwellian nature of the Raman-heated electrons. The simulation parameters were $I[\lambda_0/(1.06\,\mu m)]^2 = 2.5 \times 10^{15}$, $m_i/m_e = 100$, $l/\lambda_0 = 127$, $n/n_{cr} = 0.1$, and $T_e/T_i = 3$.
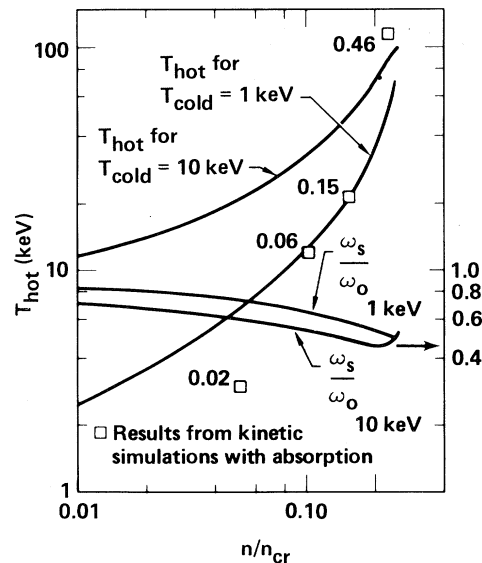
FIG. 2. Raman-backscatter–heated electron temperature, and scattered light frequency vs plasma density. The boxes are simulation results and the fraction of the light absorbed is next to the box. The lower three simulations have $I[\lambda_0/(1.06\,\mu m)]^2 = 2.5 \times 10^{15}$, $T_e = 1$ keV, $l = 127\lambda_0$, and $T_e/T_i = 3-5$. The top point has $I[\lambda_0/(1.06\,\mu m)]^2 = 10^{16}$ W/cm^2, $T_e = 10$ keV, fixed ions, and $l = 50\lambda_0$.

We find that the heated temperature is roughly independent of intensity and depends mainly on the density and background temperature which determines the phase velocity (v_p) of the Raman-generated plasma wave. In Fig. 2, we plot the heated-electron temperature versus background density for two background temperatures. The curves were found from the solution to the equations $\omega_0 = \omega_s + \omega_{epw}$, $\omega_0/c(1 - n/n_{cr})^{1/2} = \pm\,\omega_s/c(1 - \omega_{pe}^2/\omega_s^2)^{1/2} + k_{epw}$ and $\omega_{epw}^2 = \omega_{pe}^2 + 3k_{epw}^2 T_e/m_e$ (and kinetic theory[5]). Here k_{epw} is the wave number of the epw, the + (−) refers to forward scattering (backscattering).

A simple model of the backscattering in the convective regime can be given. Kinetic simulations show a rapid evolution to the nonlinear state in which the electron distribution is composed of a cold thermal Maxwellian plus a self-consistent Maxwellian tail of heated electrons, which in turn damps the plasma wave. The electron density of the tail (n_h) is determined by balancing the energy absorbed by the electrons via the damped plasma wave with the heat flux carried off by the electron tail: $rI\omega_{epw}/\omega_s \sim m_e v_p^3 n_h/2\sqrt{2}$. I is the laser intensity (W/cm^2). The epw damping is then estimated from the Landau damping rate by the heated electrons. The simple model for the convective regime is completed by computing the reflection from the damped plasma wave. The analysis is just like that for the reflection due to a damped ion wave,[6] and results in an analogous expression for the backscattered reflectivity:

$$\Lambda(1 - \Lambda) = B(\omega_0/\omega_s)\{\exp[x(1 - \Lambda)] - \Lambda\},$$

$$n/n_{cr} \lesssim 0.2,$$

where $\Lambda = (\omega_0/\omega_s)r$,

$$x = (k_{epw}^2 I/8k_s)(v_{osc}/c)^2(\omega_p/\gamma)$$
$$\times (\omega_p/\omega_{epw})(1 - n/n_{cr})^{-1/2}.$$

Here r is the fraction of light reflected, k_s is the wave number of the reflected light wave, γ is the Landau damping rate, v_{osc} is the oscillation velocity of an electron in the incident light wave $\propto \lambda_0\sqrt{I}$, c is the velocity of light, l is the length of the underdense plasma in the decay region, and B is the initial noise level of the reflected light wave.

The simple model estimates of the Raman backscatter are compared with sample simulation results in Fig. 3. Note the Raman reflectivity of order 10% was computed and the variation with the background density and temperature are in reasonable agreement with the simple model.
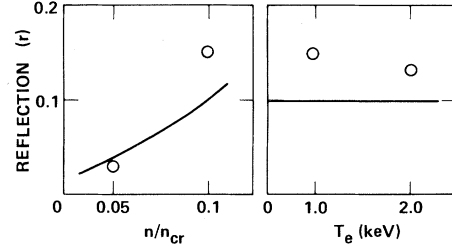
FIG. 3. Reflection due to Raman scattering as a function of the density and background temperature. The solid lines are the theoretical estimate for noise level $B = 3\times10^{-4}$ and the circles are these simulation results for $I[\lambda_0/(1.06\ \mu\text{m})]^2 = 2.5\times10^{15}$, $m_i/m_e = 100$, $ZT_e/T_i = 3$, and $l/\lambda_0 = 127$. For the left panel, $T_e = 1$ keV, and for the right panel, $n/n_{cr} = 0.1$.

Note also that rather large regions of plasma are needed to give a significant reflectivity, even neglecting the effect of gradients which are especially significant for Raman scattering as will be discussed. Hence it is not surprising that Raman scattering has only recently been observed in our experiments.

This convective model, of course, breaks down for a narrow range of densities [about $(0.2 - 0.25)n_{cr}$] where the Raman instability becomes absolute. Near quarter critical, two-dimensional (2D) effects become important. The generated plasma waves have a wider range of wave numbers and hence the heated distribution can be more complex. However, our 2D simulations show that sizable Raman scattering occurs, even in the presence of the $2\omega_{pe}$ instability, provided there is a significant region of plasma below $n_{cr}/4$. In particular, a hot plasma ($T_e = 3$ keV, $T_i = 1$ keV, $m_i/m_e = 100$) with an initial density profile rising from $0.195n_{cr}$ to $0.235n_{cr}$ in $25\lambda_0$ was irradiated by laser light with an intensity of $I\lambda_{0,\mu\text{m}}^2 = 3\times10^{15}$ W $\mu\text{m}^2/\text{cm}^2$ ($\lambda_{0,\mu\text{m}}$ is the vacuum wavelength in microns). We found net Raman scatter, absorption, and heated temperature quite comparable to the $1\frac{1}{2}$D simulation results. About 8% of the incident light was reflected with a frequency near $\omega_0/2$, compared to 13% in the $1\frac{1}{2}$D simulation. In the 2D simulation, the heated temperature was ~ 90 keV, not too far from the model estimate of 75 keV and the $1\frac{1}{2}$D simulation result (the temperature of the higher density tends to dominate the heated distribution). Finally, about 32% of the light was absorbed, emphasizing that the scattered light with frequency near $\omega_0/2$ is an underestimate of plasma heating by processes near $n_{cr}/4$, both because the $2\omega_{pe}$ is

also operative and because part of the Raman-scattered light is absorbed before exiting from the plasma. For completeness, filamentation, sidescatter perpendicular to the laser electric field, and heating by the $2\omega_{pe}$ instability deserve further attention.[7]

For $T_{cold} = 1$ keV, the growth rate of forward scatter is several times less than for backscatter. It needs a longer system, higher v_{osc}, longer time, and/or higher density to be significant. However, for large background temperatures ($\gtrsim 10$ keV), the epw wavelength of backscatter is so short that electron Landau damping tends to make backscatter less competitive relative to forward scatter. The epw associated with Raman forward scatter is typically greater than a light wavelength and becomes longer as the plasma density decreases resulting in a much higher heated-electron temperature (see Ref. 1 for graph). In simulations of $n/n_{cr} = 0.1$, $T_e = 10$, $l/\lambda_0 = 254$, and $I\lambda_{0,\mu m}^2 = 2.5 \times 10^{15}$ we have seen 25% absorption due mostly to forward scatter, with more absorption at higher densities, with energies out to several megaelectronvolts. Fortunately, the forward scatter is sensitive to the density gradient and simulations confirm the theoretical threshold:

$$I\lambda_{0,\mu m}^2 \gtrsim 5 \times 10^{17} \ (n_{cr}/\langle n \rangle)^2(\Delta n/n_{cr})\lambda_0/\Delta x,$$

where the density changes by Δn in length Δx at average density $\langle n \rangle$ (with $n/n_{cr} \lesssim 0.15$). Whereas the spectrum of backscattered light consists of mostly one peak,[5] the spectrum of forward scattering has a cascade of peaks at $\omega_0 \pm n\omega_{epw}$, where n is an integer.

To apply these results to laser-fusion-target experiments, we need to estimate the instability intensity thresholds. If the density-gradient stabilization is used to determine the intensity threshold[8] for Raman scattering, the lowest occurs at $n_{cr}/4$, and is $I[\lambda_0/(1.06 \ \mu m)]^2/10^{16} \gtrsim 35(\lambda_0/L)^{4/3} \propto \lambda_0^{-0.7}$, where $L = (n^{-1}dn/dx)^{-1}$. There is a minimum threshold intensity which occurs when L is about equal to the absorption length due to inverse bremsstrahlung. This absorption length depends on the background plasma temperature, which can be estimated in various ways. In the free-streaming flux limit, $T_e(\text{keV}) = (I\lambda_{0,\mu m}^2/5 \times 10^{13})^{2/3}$ and we obtain $I > 7 \times 10^{12} \bar{z}^{4/7}/\lambda_{0,\mu m}^{18/7}$, which is 5×10^{13} for $\bar{z} = 40$ and $\lambda_{0,\mu m} = 1$. In recent Lasnex simulations[9] with a simple model of transport inhibition, $T_e \sim 1.4 \times 10^{-6}\lambda_{0,\mu m}^{0.4}I^{0.4}\bar{z}^{0.3}\tau^{0.4}$, where τ is the pulse length in nanoseconds. For this temperature scaling the backscatter threshold becomes $I > 1.4 \times 10^{13}\bar{z}^{-0.4}\lambda_{0,\mu m}^{-2.3}\tau^{-0.4}$ which is
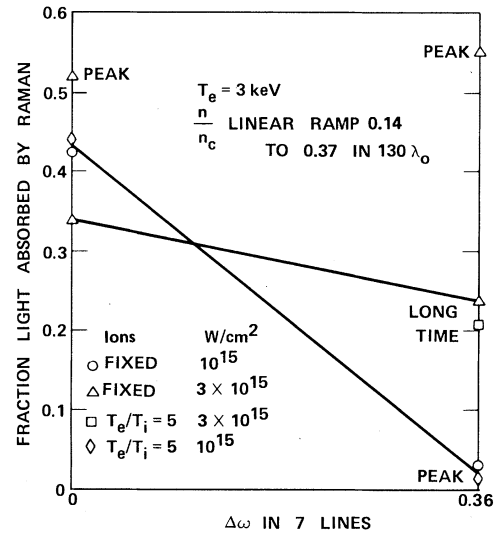
FIG. 4. Fraction of the light absorbed by Raman vs bandwidth of the laser for several total laser intensities. The simulation plasma had $130\lambda_0$ from densities $0.14n_{cr}$ to $0.37n_{cr}$.

again 6×10^{13} W/cm^2 for $\bar{z} = 40$, $\tau = 1$ nsec and $\lambda_{0,\mu m} = 1 \ \mu m$.

If laser-fusion experiments are close to the intensity threshold, Raman scattering can be decreased by the use of laser light with a large bandwidth $\Delta\omega$ as is shown in Fig. 4. The $\Delta\omega$ was chosen to be the same as is projected for an experiment on the Cyclops laser[10]: seven lines of equal intensity separated by 6% for total width of 36%. When the growth rate is less than the line separation, one expects each line to behave independently. The linear growth rate $n_{cr}/4$ was $0.06\omega_0$ for the higher intensity shown which is about equal to the line separation. At early times the bandwidth does not decrease the reflection and heating, but later when the self-consistent heating provides some damping, there is an improvement. For lower intensity, where the line-width is greater than the growth rate, the Raman instability is essentially driven below the ∇n threshold. Hence $\Delta\omega$ seems effective in reducing the Raman instability near threshold.

In summary we have modeled Raman backscatter and forward scatter in the convective regime and have evaluated density gradients and bandwidth as means for avoiding the deleterious effects of these instabilities for laser-fusion applications.

[1]Don Phillion, to be published.
[2]J. Elazar, W. Toner, and E. R. Wooding, private communication.

[3]C. S. Liu, M. N. Rosenbluth, and R. B. White, Phys. Fluids 17, 121 (1974); D. W. Forslund, J. M. Kindel, and E. L. Lindman, Phys. Fluids 18, 1002 (1975); W. Manheimer and H. Klein, Phys. Fluids 17, 1889 (1974); B. I. Cohen, A. N. Kaufman, and K. M. Watson, Phys. Rev. Lett. 29, 581 (1972); Kent Estabrook, D. Phillion, and V. Rupert, Lawrence Livermore Laboratory Laser Fusion Monthly Report, June 1979 (unpublished); W. L. Kruer, K. G. Estabrook, and K. H. Sinz, Nucl. Fusion 13, 952 (1973); J. J. Thomson, Phys. Fluids 21, 2082 (1978); T. Tajima and J. M. Dawson, Phys. Rev. Lett. 43, 267 (1979).
[4]J. F. Drake and Y. C. Lee, Phys. Rev. Lett. 31,

1197 (1973).
[5]W. L. Kruer, K. G. Estabrook, B. F. Lasinski, and A. B. Langdon, Phys. Fluids 23, 1326 (1980).
[6]D. W. Phillion, W. L. Kruer, and V. C. Rupert, Phys. Rev. Lett. 39, 1529 (1977).
[7]A. B. Langdon, B. F. Lasinski, and W. L. Kruer, Phys. Rev. Lett. 43, 133 (1979); A. B. Langdon and B. F. Lasinski, Phys. Rev. Lett. 34, 934 (1975); D. W. Forslund, J. M. Kindel, and K. Lee, to be published.
[8]M. N. Rosenbluth, Phys. Rev. Lett. 29, 565 (1972).
[9]M. Rosen et al., Phys. Fluids 22, 2020 (1979), and private communication.
[10]D. Eimerl, private communication.

Observation of an Upper-Hybrid Soliton

Teruji Cho and Shigetoshi Tanaka
Department of Physics, Faculty of Science, Kyoto University, Kyoto 606, Japan
(Received 30 May 1980)

A density cavity at the upper-hybrid resonance layer has been observed in the saturated stage of the trapped electrostatic field when a high-power microwave of the extraordinary mode is injected into an afterglow plasma column in a uniform magnetic field. The results can be explained by the modulational instability at the upper-hybrid frequency and the formation of an upper-hybrid soliton.

In the absence of a magnetic field the density cavity near the electron plasma frequency ω_{pe} has been extensively studied.[1-4] In the presence of a magnetic field some aspects of the nonlinear modulation of the upper-hybrid wave have been examined theoretically.[5-8] Porkolab and Goldman[5] predicted that a high-power microwave forms an upper-hybrid envelope soliton. Such a phenomenon is worthy of study, since this effect may occur both in the electron cyclotron heating of toroidal plasmas[9-12] and also in laser-plasma interaction.[13] In this Letter we report the first experimental observation of a density cavity in the saturation stage of modulational instability at the upper-hybrid resonance (UHR) layer in a plasma column in a magnetic field.

The experiments were carried out in a linear machine. A vacuum vessel (11 cm in diameter, 125 cm in length) is located in a uniform magnetic field B (<3.5 kG). The pulsed dc discharge is produced at an argon gas pressure of $p = (5-10) \times 10^{-4}$ Torr by using an oxide cathode (3 cm in diameter). The experiments are performed in an afterglow plasma, whose typical parameters are an electron temperature $T_{e0} \approx 2.5$ eV and an elec-

tron density $n_{e0} \approx 2 \times 10^{12}$ cm^{-3} at the center of the positive column. A high-power microwave ($\omega/2\pi = 9.4$ GHz, $P_\mu \lesssim 50$ kW and $\tau_\mu = 0.3-1.5$ μs) is injected into the plasma in the form of the extraordinary mode with use of a standard waveguide, whose end is located at $r = 5.5$ cm from the center of the plasma column.

In Fig. 1(a) the radial profiles of the wave intensity I_μ and the electron density n_e are plotted when the low P_μ is injected from the left-hand side of the plasma column. The intensity I_μ is picked up by the probe located in front of the waveguide and sampled by a boxcar integrator. The incident microwave, passing the cyclotron cutoff, tunnels through the evanescent region and arrives at the UHR layer ($\omega = \omega_{UH}$), where it is converted to the electron Bernstein mode (EBM) which propagates towards the high-density region. This behavior is well known in the linear theory.[14-17] However, when a high P_μ is injected, an electron density depression (cavity, whose half-width is 3-4 mm,) is observed at the UHR layer [Fig. 1(b)]. The injected microwave seems to be trapped at the UHR layer, since the intensity I_μ at $\omega = \omega_{UH}$ increases drastically, while that of